

21. SEISMIC VELOCITIES AT SITE 891 FROM A VERTICAL SEISMIC PROFILE EXPERIMENT¹

G.F. Moore,² J. Dellinger,^{2,3} M.E. MacKay,² and H. Hoskins⁴

ABSTRACT

A vertical seismic profile experiment carried out at Ocean Drilling Program Site 891 ties the regional seismic reflection data to the drilled and logged section and provides additional velocity data near the frontal thrust. The depth of the frontal thrust is confirmed to be between 425 and 440 mbsf at a two-way traveltime of 4.05 s. Compressional *P*-wave velocities in the upper 275 mbsf as determined by a walkaway VSP (1883 m/s) are consistent with those measured by in situ wireline sonic logs. Sonic log velocities between 310 and 400 mbsf are bounded by the walkaway VSP (1883 to 1835 m/s) and zero-offset VSP (2193 m/s) velocities. Below the depth of the drill hole, the walkaway VSP velocities are significantly lower than those determined by stacking velocity analyses on nearby multichannel seismic lines. Shear wave velocities in the upper section, as measured by the walkaway VSP, are about 340 m/s.

INTRODUCTION

Synergistic interactions of fluids and deforming rocks are the dominant control on the structural evolution of accretionary prisms. Difficulties in determining the interrelationships among the physical properties of the sediments undergoing deformation hampers our understanding of the mechanics of accretionary processes. Porosity loss through consolidation and cementation reduces rock permeability and increases strength, which in turn alters the deformational style. Direct measurements of porosities in accretionary prisms are difficult to make, so we have been forced to use seismic velocity as a proxy for porosity (e.g., Bray and Karig, 1988; Hyndman et al., 1993; Cochran et al., 1994b). Although easier to measure than in situ porosity, seismic velocity is also difficult to define accurately in the complex structural environments of subduction zones. One of the objectives of Ocean Drilling Program (ODP) Leg 146 was to determine the velocity structure at the toe of the Oregon margin accretionary prism by collecting in situ logs and vertical seismic profiles (VSPs). The VSP experiment proposed for Site 891 was designed to tie the drilled section to the regional multi-channel seismic reflection (MCS) data (Fig. 1), to obtain bounds on interval velocities and time-depth functions above the frontal thrust. Both zero-offset and walkaway VSPs were conducted in Hole 891C. In this paper we report the results of this VSP experiment.

In a zero-offset VSP, the seismic wavefield generated by a source at the surface directly above the hole is recorded by a seismometer clamped in the borehole at different depths (Gal'perin, 1974; Balch and Lee, 1984; Hardage, 1983). For a walkaway VSP, the seismometer is clamped at a single position while the surface source is fired as it is moved (walked) away from the borehole. Offsetting the source with respect to the downhole geophone causes a movement of reflection points away from the well. A walkaway VSP illuminates the zone below the geophone, thereby imaging the structure below and laterally away from the borehole (e.g., Kennett et al., 1980).

ZERO-OFFSET VSP

Data Acquisition

The zero-offset VSP used a 4.92-L (300-in³) air gun. At least six shots were fired at every VSP station. Shot breaks were received by a hydrophone suspended just beneath the guns and a second hydrophone suspended approximately 150 m below the guns.

Seismic signals were received by a Geospace wall-lock seismometer, which contained three pairs of 4.5-Hz geophones (Bolmer et al., 1992). Each pair is wired in series and orthogonally configured with two components in the plane normal to the borehole and one parallel to the borehole. The orientation of the horizontal phones is not known. The near-critically damped geophones have a flat response from 4.5 to 100 Hz. During the zero-offset VSP, 24 geophone clamping stations were occupied from 453 mbsf to 325 mbsf at 5-m intervals. Adequate clamping was not possible in the interval from 425 to 440 mbsf because of poor hole conditions. The horizontal components of the zero-offset VSP are unusable because of an electrical problem with the downhole tool.

The signals from the three seismic channels were high-cut filtered at 120 Hz and digitized at 2-ms sample interval (500 Hz). The digital data were recorded in SEG-Y format on magnetic tape on a workstation.

Data Processing

The zero-offset VSP data were processed to reduce noise and to separate the upgoing and downgoing wavefields. We followed standard processing procedures (e.g., Balch and Lee, 1984; Hardage, 1983). Because of inconsistent triggering from the shot break hydrophone, all shot times were first referenced to the deep hydrophone to achieve a stable datum for stacking; a correction for the hydrophone depth was later added to move the reference to sea level. The deep hydrophone data were interpolated to 1 ms sample interval and shot break times were read to the nearest millisecond. After correcting for shot-break times, each shot was band-pass filtered (6-10-55-64 Hz), plotted, and visually inspected. Excessively noisy shots were deleted. The remaining shots for each depth were then summed and displayed (Fig. 2). The most prominent event arrivals are the direct arrivals (first breaks) and the following air-gun bubble pulse. The data were interpolated to 1 ms sample interval and first break times were picked to the nearest ms. After first break times were subtracted from each trace to shift the traces to zero time, a 15-point median filter was applied to enhance the downgoing wave field. The downgoing wave en-

¹Carson, B., Westbrook, G.K., Musgrave, R.J., and Suess, E. (Eds.), 1995. *Proc. ODP, Sci. Results*, 146 (Pt. 1): College Station, TX (Ocean Drilling Program).

²Department of Geology and Geophysics, University of Hawaii, Honolulu, HI 96822, U.S.A.

³Present address: Amoco Tulsa Research Center, Tulsa, OK 74103, U.S.A.

⁴Department of Geology and Geophysics, Woods Hole Oceanographic Institution, Woods Hole, MA 02543, U.S.A.

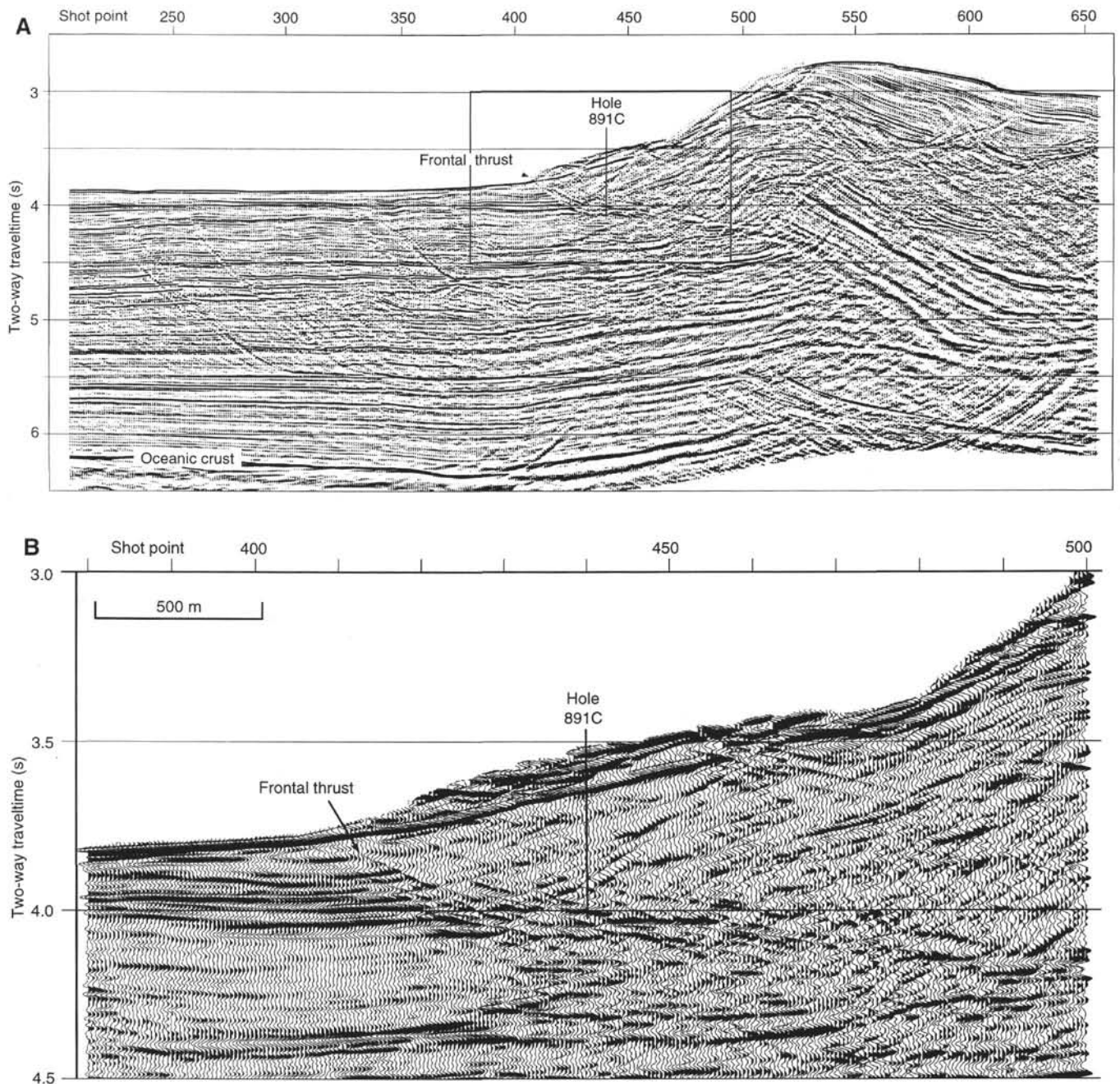


Figure 1. Regional seismic line OR8905 across the toe of the Oregon accretionary prism. The line passes east-west, directly over Site 891. The line has been stacked and depth-migrated but is displayed in two-way traveltime for better correlation with the VSP data. Hole 891C penetrated through the toe of the prism into the frontal thrust. Length of (A) corresponds to length of walkaway VSP data displayed in Figures 7 and 8. Box in (A) shows location of enlargement in (B).

ergy was then subtracted from the total wave field to yield the upgoing wave energy. An inverse deconvolution filter was then designed on the downgoing wave field and applied to the upgoing wavefield. Twice the first-break time was then added to this deconvolved data set to shift it to two-way traveltime. A 5-point median filter was then applied to further enhance the upgoing wavefield (Fig. 3). All horizontal wave energy in this display should represent wavetrains reflected from horizons below the geophone. The VSP traces were then stacked to produce a composite trace for comparison to the MCS data (Fig. 4).

Comparison to Regional Seismic Reflection Data

The stacked zero-offset VSP data should be directly comparable to the regional MCS data. Figure 4 shows two duplicate traces of the stacked VSP compared to the migrated seismic reflection data from line OR8905. Because of the different deconvolution schemes applied to the VSP and MCS data, the VSP data appear to be higher frequency, but the major reflections still correlate between the two data sets. A reflection in the VSP data at about 4.05 s correlates with the frontal thrust reflection, indicating that the frontal thrust was inter-

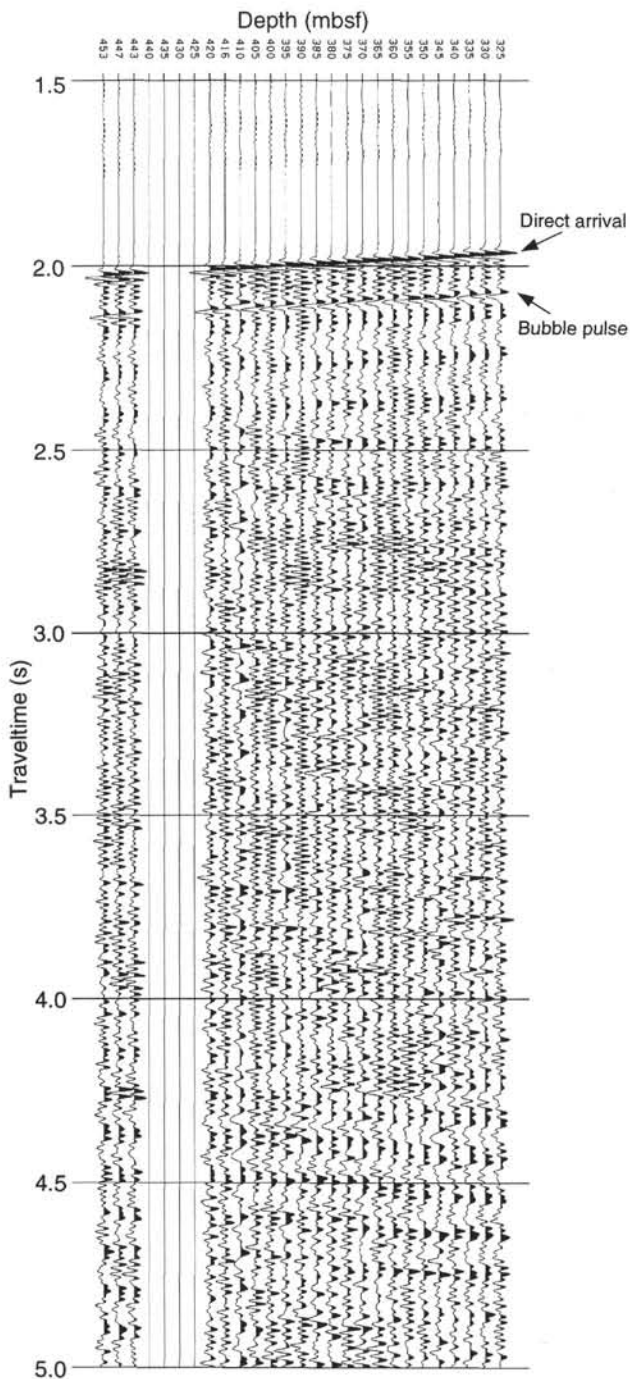


Figure 2. Filtered and stacked traces of air-gun zero-offset VSP. Blank traces have been added to reserve depth spacing across zone of no data.

sected by the VSP in the “no data” interval between 420 and 440 mbsf. This is consistent with core data that are interpreted to show the frontal thrust to be at 437 mbsf (Shipboard Scientific Party, 1994) and probably indicates that the hole was unstable at the frontal thrust, making clamping of the seismometer impossible. Note that the frontal thrust reflection in the VSP data is negative polarity and therefore correlates with the lower splay identified by J.C. Moore et al. (this volume), although the time of this reflection is about 10 ms shallower in the VSP data than in the MCS data. This discrepancy may be because the drill site is not exactly on the MCS line.

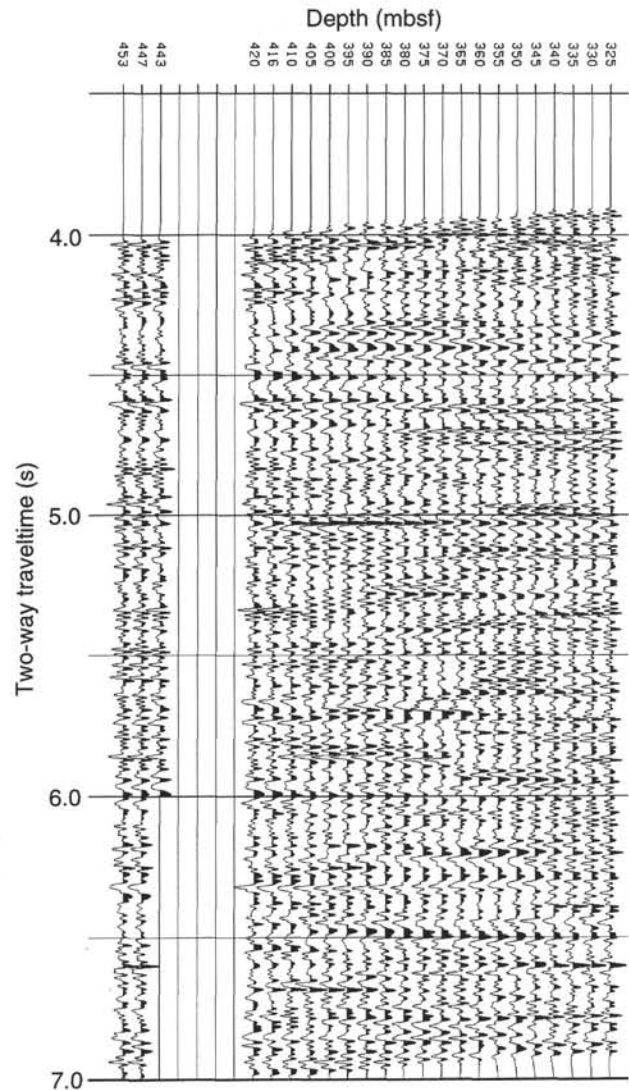


Figure 3. Upgoing wavefield of the zero-offset VSP converted to two-way traveltimes. Wavefield has been deconvolved and median filtered to enhance the upgoing waves.

A strong reflection at about 4.6 s correlates with a strong reflection on the seismic line. The VSP reflections at about 6.1–6.2 s correlate with the oceanic crust reflection, but they are much sharper than the oceanic crust reflection on the MCS data, probably because of the deconvolution applied to the VSP data. Other reflections above the oceanic crust are difficult to exactly correct between the reflection and VSP data.

Velocity Analysis

The first-break times from the zero-offset VSP (Fig. 5) provide a time-depth profile for the sampled interval. Velocities were determined by fitting line segments to the data points via least-squares linear regression. Although shorter intervals with different velocities can be obtained, the best fit to the data is a single velocity of 2193 ± 55 m/s for the interval sampled by the zero-offset VSP (453 to 325 mbsf). We note that the first arrival times could be in error by ± 1 ms because of low signal-to-noise levels and inaccuracies in picking both first-break times and shot-break times. Additional errors result

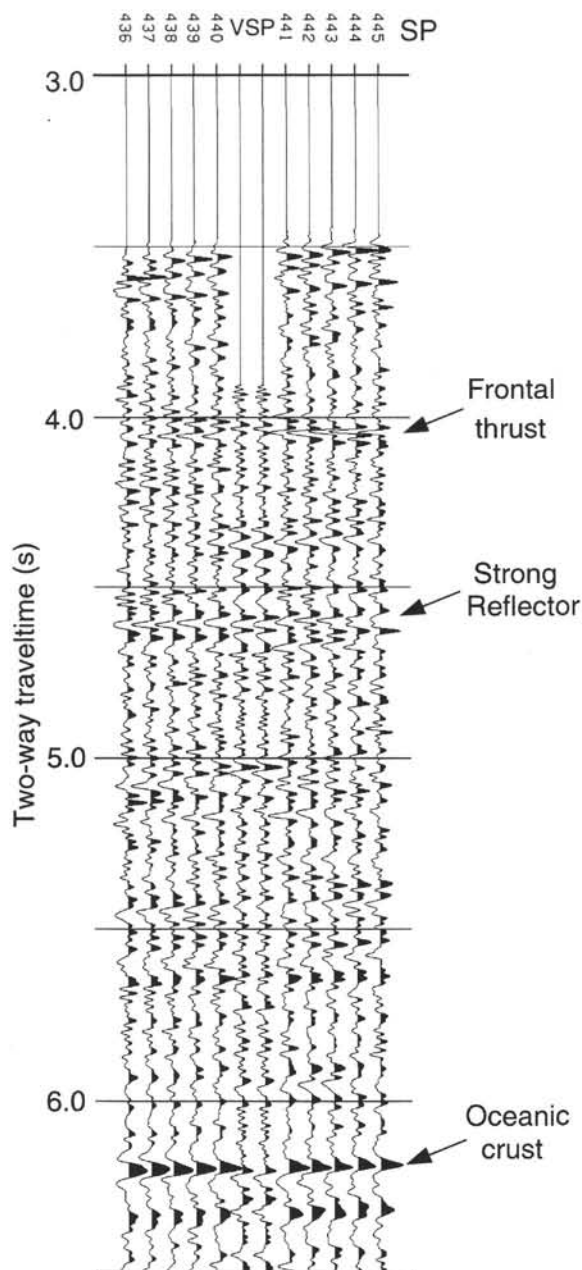


Figure 4. Stacked VSP traces displayed adjacent to traces from regional seismic reflection line OR8905. VSP shows location of VSP traces; SP refers to shot point numbers of reflection line.

from mislocation of the seismometer depth (estimated to be ± 1 m). We estimate total errors in this analysis to be $\pm 2-3\%$.

WALKAWAY VSP Data Acquisition

The seismic signals for the walkaway VSP were generated by an array of three air guns (4.92, 2.46, 1.3 L; 300, 150, 80 in³) fired by the *New Horizon* with the geophone clamped at a single position in the borehole. Two lines were run: line 1 from west to east and line 2 from south to north (Fig. 6). The walkaway VSP used a different Geospace seismometer than that used in the zero-offset VSP, but its character-

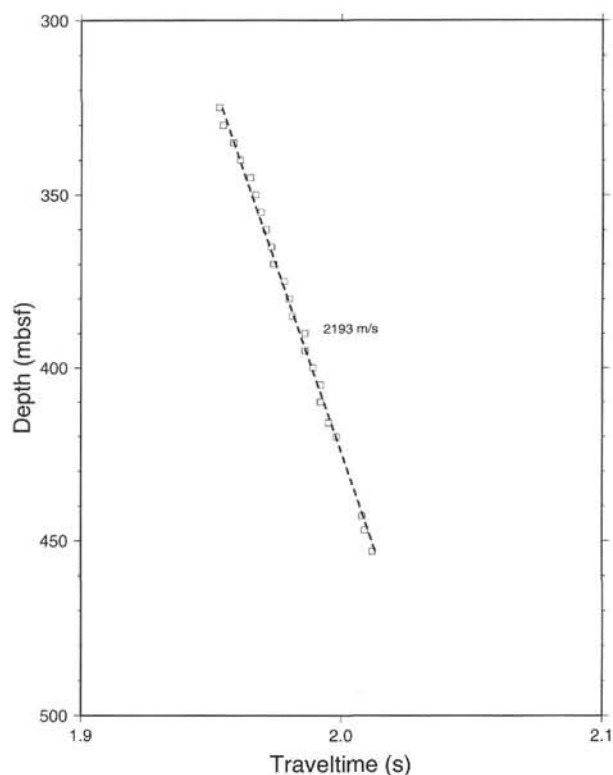


Figure 5. Traveltime vs. depth of first breaks picked from the zero-offset VSP. Dashed line shows least-squares fit used to determine velocities.

istics were the same except that it did not have the electrical short which prevented recovery of horizontal information for the zero-offset VSP. During the walkaway VSP, the geophone was not well clamped in the uncased hole, severely distorting the particle-motion direction information we had hoped to recover. Although three clamping stations were occupied during the walkaway VSP, hole problems and mechanical difficulties severely degraded the data collected at two of the stations. Here we discuss only the data acquired with the seismometer clamped at 273 mbsf. The seismic signals were recorded on the drill ship using the same system as was used for the zero-offset VSP. Because of the increased noise during the walkaway VSP, the high-cut filter was set at 100 Hz. Digitization and recording were at 2 ms (500 Hz).

Navigation of the *New Horizon* was by global positioning system (GPS). The *JOIDES Resolution* also acquired GPS data during the walkaway VSP, so we were able to correct the dithered GPS locations by subtracting out the introduced errors based on the drill ship's position. The shot interval was 15 s, giving a nominal shot spacing of 37.5 m, but our post-cruise processing shows that the actual shot spacing varied from 31 to 45 m.

The extent of the walk-away VSP shots in the dip direction (line 1) corresponds to the portion of MCS line OR5 displayed in Figure 1A. Note the extreme topographic variations along the line.

Data Processing

During the walkaway VSP the recording gain was changed as the shooting ship's range changed. This required removal of the gain changes during processing. Amplitudes were then multiplied by t^2 to correct for spherical spreading. The plots in Figures 7-10 have an additional scale of amplitude to the 0.7 power to boost weak vs. strong events. The walkaway VSP data were contaminated by a large noise spike at 70 Hz. To remove it, we bandpass filtered the data using a 6-

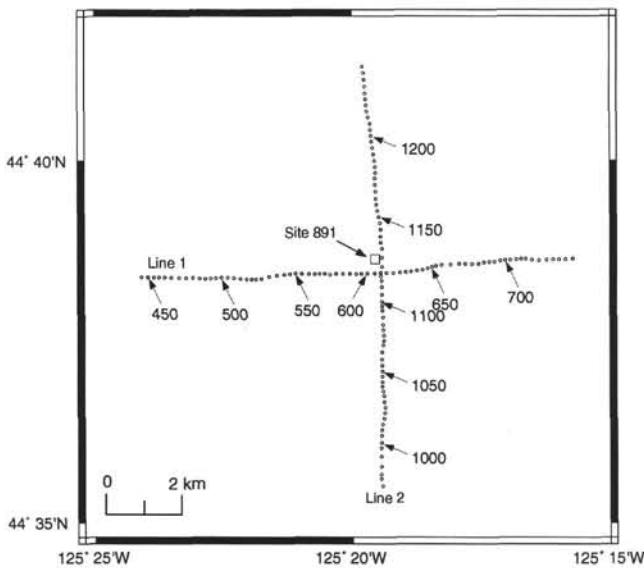


Figure 6. Location of walkaway VSP shots relative to Site 891. Circles are locations of shots on even minutes (every fourth shot).

pole filter, with -6 db points at 0 and 60 Hz. The output was then decimated by a factor of 2 to a 0.004-s sample rate. The filtered data set (Fig. 7A) shows that the south-to-north line (line 2), which was shot second, was much noisier than the west-to-east line (line 1), indicating that the quality of the borehole was deteriorating during the VSP experiment.

All three components of the geophone were working during the walkaway VSP, but the signal was corrupted by poor coupling between the geophone and the hole. The polarization of the direct P -wave arrival should have been approximately linear and tracked the source-receiver direction as the source moved about. Polarization analysis of the first arrival in the bandpassed data instead showed elliptical polarizations that varied with source position in a complex way. We will briefly describe the technique used to “unscramble” the data. A more complete description will be published elsewhere (Delinger, unpubl. data).

Unscrambling the true particle motion is a vector deconvolution problem. We need to solve the system

$$\mathbf{MD} \times \mathbf{L} \approx 0,$$

where \mathbf{D} is a 3-vector of traces from the recorded data, windowed about the first arrival; \mathbf{M} , a vector deconvolution operator, is the 3-by-3 matrix of traces we need to determine (\mathbf{MD} is the corrected data); \mathbf{L} is the 3-vector giving the assumed linear polarization direction (a vector pointing from the receiver to the source); and ≈ 0 is in the least-squares sense, summed over all times and source positions. Note if the corrected data were always exactly linearly polarized in the source-receiver direction, $\mathbf{MD} \times \mathbf{L}$ would be zero for all times and source positions, and exact equality would be achieved.

In practice, more constraints are necessary, because any solution for the unscrambling operator \mathbf{M} is equally good after arbitrary time shift. We want to find a *causal* solution; therefore, we constrain \mathbf{M} to have the following form: \mathbf{M} is zero before time zero. At time zero, \mathbf{M} has unit energy (sum of the squares of the 9 0-lag elements of \mathbf{M} is 1). After time zero there is a “gap” during which \mathbf{M} again is constrained to be 0. (For our example the gap was 1 sample point long.) After the gap (until some specified maximum filter length), \mathbf{M} is unconstrained. (In our example the total filter length, including the 0 lag

and the gap, was 25 samples.) This corresponds to a least-squares problem with quadratic constraints.

Unscrambling the data properly corrects the very first arrival direction, but any extended oscillations of the geophone due to the poor clamping will be ignored. To fix that we need to do vector deconvolution. This is similar to standard scalar deconvolution, except we allow one component to predict another. In vector deconvolution, we find a 3-by-3 matrix of traces \mathbf{F} such that

$$\mathbf{FD} \approx 0,$$

where \mathbf{F} is the filter we are trying to find, \mathbf{D} is the 3-vector input data, and \mathbf{FD} is the deconvolved data. The ≈ 0 is again in the least-squares sense, summed over source position and time. \mathbf{F} is constrained to be the identity matrix at time zero, then 0 for the duration of some gap, and then is unconstrained for later lags.

For our example these processing steps had some beneficial effect, but they could not recover the complete particle motion; much of the three-component information was too deep in the noise to recover. Figure 7B shows the vertical component after filtering, unscrambling, and vector deconvolution. Many strong arrivals are seen, but additional processing is necessary prior to interpretation.

We then mathematically rotated the three-component data to represent three distinct directions of possible particle motion (Fig. 8). The P response is a vector from source to receiver, so it points in the direction of the P -wave first arrival. SV and SH are two mutually orthogonal particle displacements that are perpendicular to the P vector, with SV being a vector in the vertical plane containing the source and receiver (Hardage, 1983). Note the polarity reversal on the SV and SH components as the shots pass the geophone location.

Velocity Analysis

For the walkaway VSP, we had incomplete particle-motion direction information and only a single good depth location, so we were only able to do a simple Dix-style velocity analysis. For nondipping plane layers a walkaway VSP survey is kinematically similar to a common midpoint gather, but with layers above the geophone traversed only once instead of twice. If the layers are dipping, however, the situation becomes more complicated. In a standard common-midpoint surface survey, the reflection point moves updip as offset is increased and the moveout velocity is higher than it would be for a horizontal reflector. For a VSP, the velocity does not increase; instead, the top of the three-dimensional hyperbola is offset away from the drill hole. Instead of the familiar moveout equation

$$T^2 = T_0^2 + (x/v)^2,$$

we must use

$$T^2 = T_0^2 + (|X - X_0|/v)^2,$$

where X is the source position vector and X_0 is the vector location of the top of the hyperbola (earliest arrival). We must simultaneously find both moveout velocity (in meters per second) and the offset X_0 (in meters). If the arrival of interest cannot be followed over a sufficient span of shot locations, or is distorted due to lateral heterogeneity, it may not be possible to determine both of these independently.

Note that an offset perpendicular to the recording line merely causes the earliest arrival to be later, confusing any attempt to generate interval velocities from moveout velocities. However, if there is sufficient three-dimensional source-location coverage, the map location of the hyperbola top can be determined, and the ambiguity between T_0 and hyperbola offset disappears.

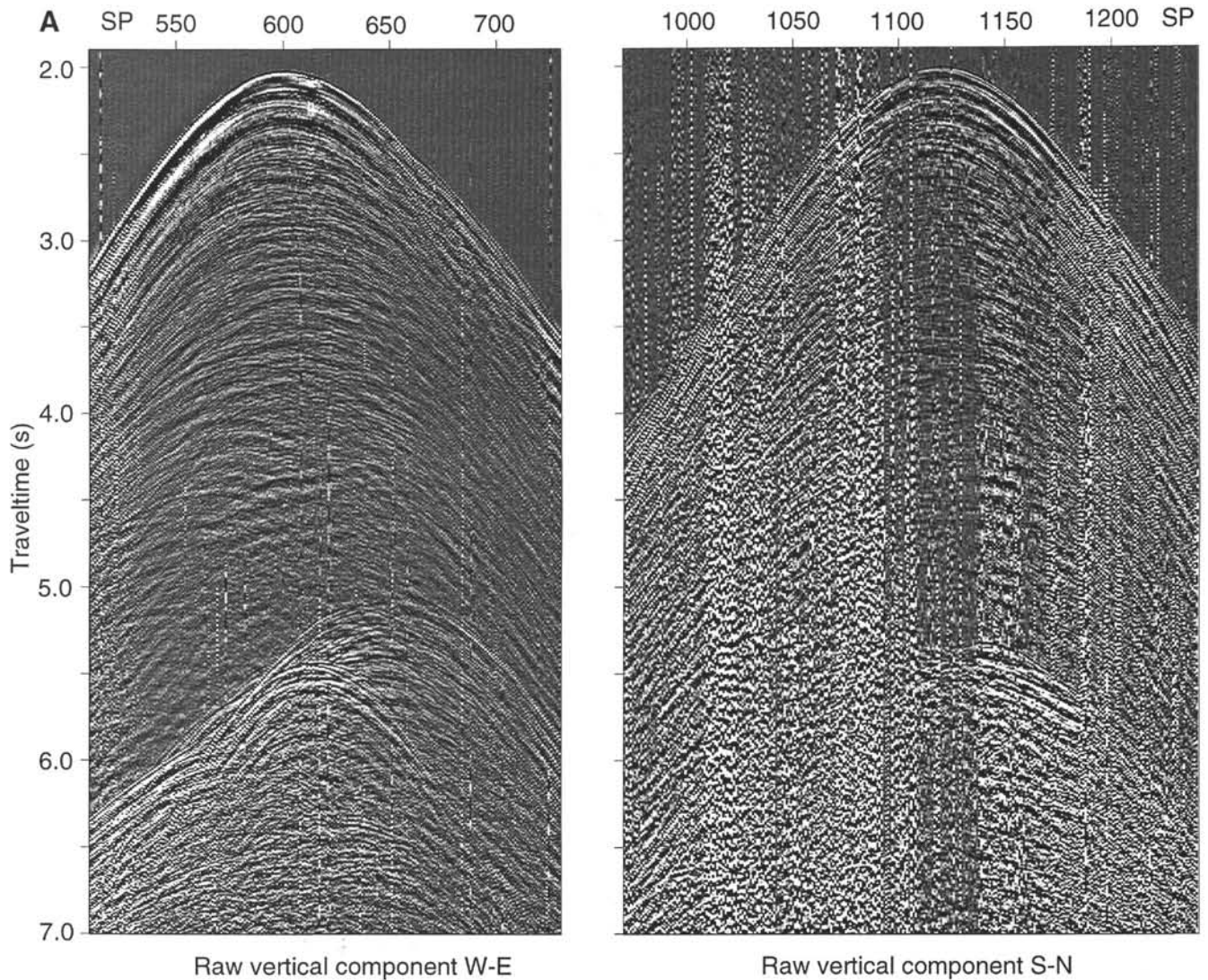


Figure 7. Vertical component of walkaway VSP data. **A.** After band-pass filter only. **B.** After filter, unscrambling, and vector deconvolution.

A more insidious problem is that while each event provides a root mean square (RMS) velocity, it is an RMS velocity averaged along the minimum traveltime raypath for that event. If the X_0 are different, the raypaths are different, and the various RMS velocities determined for different events cannot be directly compared to find interval velocities.

The complex 3D structure in the neighborhood of the drill site (Fig. 1) makes it difficult to measure accurate "interval velocities," but approximate velocities can be found using the few continuous events. Because of the complex seafloor topography, numerous energy paths are possible; for example, the "direct P -wave" arrives multiple times between 2.0 and 2.2 s (Fig. 9A). Most of the strong events deeper in the record prove to have moveout velocities of around 1525 m/s (but with a wide variation in offsets). These are water bottom multiples; two encounters with the complex seafloor allows for an even greater variety of energy paths.

Given these caveats, it is possible to find an approximate velocity profile using the walkaway VSP data. Note three parameters are required to account for the moveout of the events: a standard moveout velocity (in meters per second), a displacement of the hyperbola top to the east (in meters), and a displacement of the hyperbola top to the

north (in meters). To some extent these parameters interact, making it difficult to fit precise velocities. The velocities determined from the walkaway VSP are shown in Table 1. Examples of several events with RMS velocities applied are shown in Figure 9.

One event at 5.4 s is particularly interesting. It is difficult to pick out among the first-order seafloor multiples, but it is distinguishable by its very different moveout velocity (Fig. 9E and F). The moveout velocity of 900 m/s is considerably slower even than that of seawater, implying an RMS velocity in the sediment of 340 m/s along this raypath. Although the horizontal components of the three-component geophone are not well resolved, this event is also anomalously strong on the deconvolved " SH " section, indicating a different particle-motion direction than the P -wave arrivals. This event is probably a shear wave; unfortunately, there is insufficient horizontal information even after the vector deconvolution to allow a meaningful investigation of shear-wave splitting.

To find a true shear velocity we need to know more about the raypath, particularly at what point along the raypath the conversion from P to S occurred. The late arrival, 3 seconds after the direct P -wave, indicates that either the shear-wave velocity must be considerably slower than the upper limit of 340 m/s, or the shear portion of the ray-

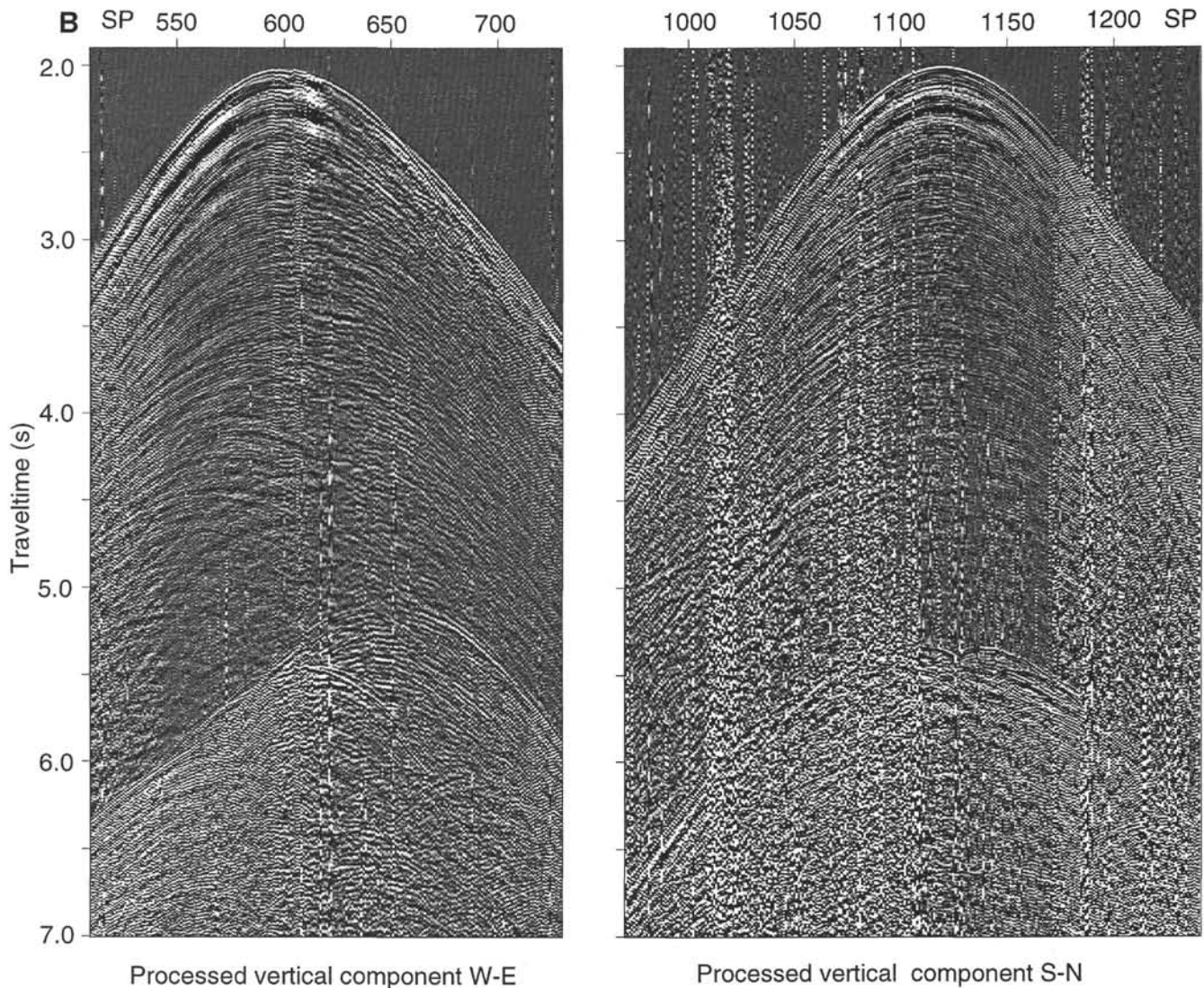


Figure 7 (continued).

path must be longer than that for a direct arrival with a *P*-to-*S* conversion at the seafloor. The hyperbola-top offset of 250 m north and 250 m east does indicate that the raypath cannot be completely vertical. Without further information, we can only conclude that, whatever the raypath, the shear wave velocity in the sediment must be quite slow, less than 340 m/s.

Errors in these velocity measurements are caused by mispicking of event times (± 1 ms), mislocation of the depth of the receiver (± 1 m), and performing velocity analyses at 50 m/s intervals. Even in the flat-layer case, the reflection point in a walkaway VSP varies with offset. As a result, reflector inhomogeneities that would only cause reflector-depth variations between different common-midpoint stacks instead disrupt the hyperbolic moveout on a walkaway VSP. In addition, errors are introduced during the conversion of RMS to interval velocities. We therefore estimate that the potential errors in the walkaway VSP velocities could be as high as $\pm 10\%$ – 12% .

DISCUSSION

Figure 10 is a comparison of the available velocity data at Site 891. We compare the corrected long-spaced sonic log data (Ship-

board Scientific Party, 1994) and interval velocities from the regional MCS lines (Cochrane et al., 1994b) with our VSP *P*-wave velocity data. Velocities in the upper 275 mbsf as determined by the walkaway VSP (1883 m/s) are consistent with those measured by the in situ wireline sonic logs. Sonic log velocities between 310 and 400 mbsf are bounded by the walkaway VSP (1883 to 1835 m/s) and zero-offset VSP (2193 m/s) velocities. The log velocities being lower than the zero-offset VSP velocities may be because of degradation of the hole prior to logging. The sonic log measures velocities close to the hole whereas the VSP measures velocities over a much larger area. Below the depth of the drill hole the walkaway VSP velocities are significantly lower than those determined by stacking velocity analyses. We note that the MCS velocities must be too high below the frontal thrust at this location because footwall strata below the frontal thrust dip too steeply landward in the section converted from time to depth using the MCS velocities by Cochrane et al. (1994a).

ACKNOWLEDGMENTS

This work was supported by the National Science Foundation through grant OCE-9116041. Data acquisition was funded by grants

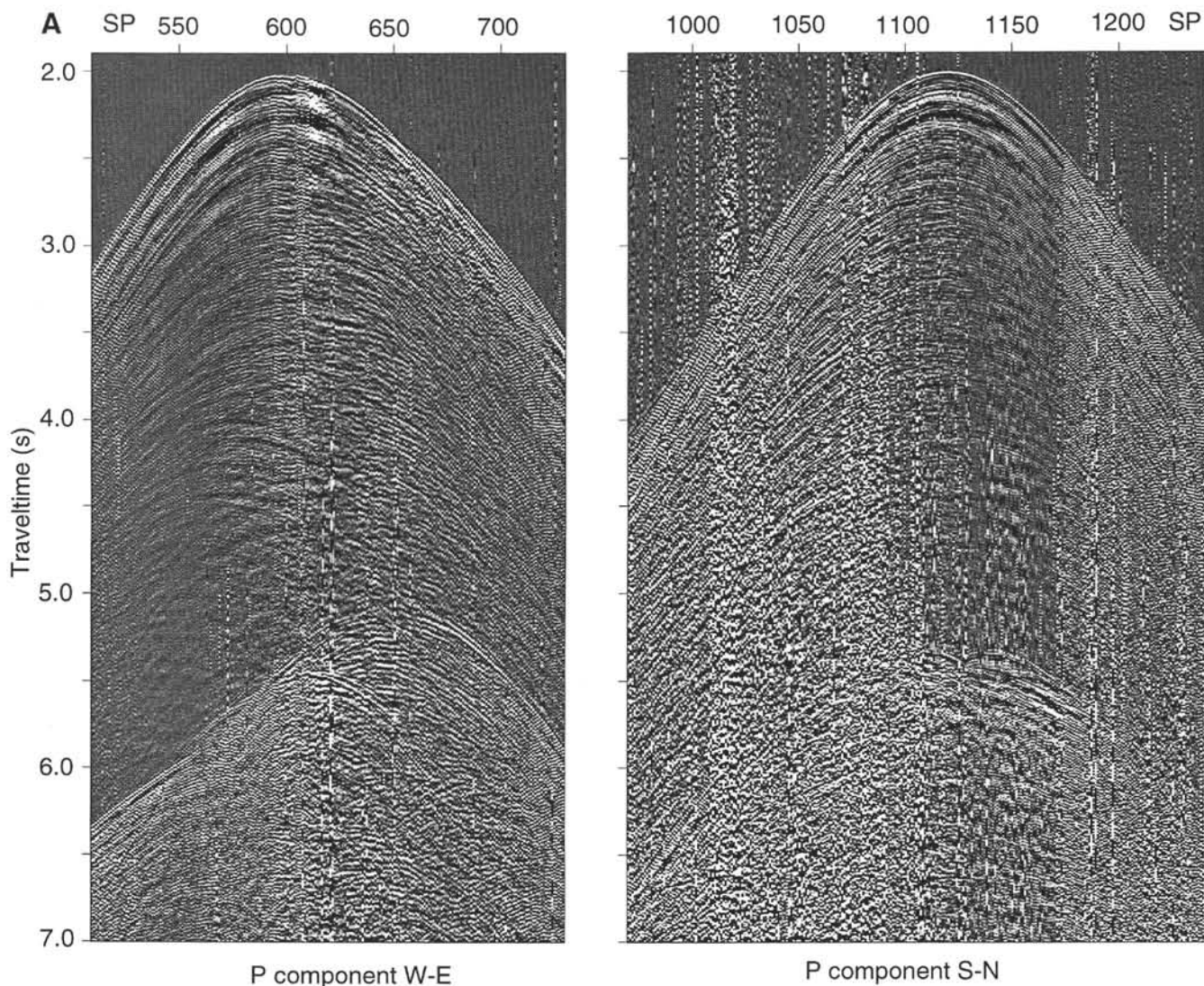


Figure 8. Walkaway VSP data after rotation to track the P -wave first arrival. **A.** P -wave particle motion. **B.** SV particle motion. **C.** SH particle motion.

from JOI/USSAC to WHOI and UH. MacKay was supported by a JOI/USSSP post-cruise grant. We thank Zhiyong Zhao for assistance in processing the zero-offset VSP. Roy Wilkens reviewed an early draft of the manuscript. SOEST contribution number 3824.

REFERENCES

- Balch, A.H., and Lee, M.W. (Eds.), 1984. *Vertical Seismic Profiling: Techniques, Applications, and Case Histories*: Boston (Int. Human Resour. Develop. Corp.).
- Bolmer, S.T., Buffler, R.T., Hoskins, H., Stephen, R.A., and Swift, S.A., 1992. Vertical seismic profile at Site 765 and seismic reflectors in the Argo Abyssal Plain. In Gradstein, F.M., Ludden, J.N., et al., *Proc. ODP, Sci. Results*, 123: College Station, TX (Ocean Drilling Program), 583–600.
- Bray, C.J., and Karig, D.E., 1988. Dewatering and extensional deformation of the Shikoku Basin hemipelagic sediments in the Nankai Trough. *Pure Appl. Geophys.*, 128:725–747.
- Cochrane, G.R., MacKay, M.E., Moore, G.F., and Moore, J.C., 1994a. Consolidation and deformation of sediments at the toe of the central Oregon accretionary prism from multichannel seismic data. In Westbrook, G.K., Carson, B., Musgrave, R.J., et al., *Proc. ODP, Init. Repts.*, 146 (Pt. 1): College Station, TX (Ocean Drilling Program), 421–426.
- Cochrane, G.R., Moore, J.C., MacKay, M.E., and Moore, G.F., 1994b. Velocity and inferred porosity model of the Oregon accretionary prism from multichannel seismic reflection data: implications on sediment dewatering and overpressure. *J. Geophys. Res.*, 99:7033–7043.
- Gal'perin, E.I., 1974. *Vertical Seismic Profiling*. Spec. Publ.—Soc. Explor. Geophys., 12.
- Hardage, B.A., 1983. *Vertical Seismic Profiling, Part A. Principles*: London (Geophysical Press).
- Hyndman, R.D., Wang, K., Yuan, T., and Spence, G.D., 1993. Tectonic sediment thickening, fluid expulsion, and the thermal regime of subduction zone accretionary prisms: the Cascadia margin off Vancouver Island. *J. Geophys. Res.*, 98:21865–21876.
- Kennett, P., Ireson, R.L., and Conn, P.J., 1980. Vertical seismic profiles: their application in exploration geophysics. *Geophys. Prospect.*, 28:676–699.
- Shipboard Scientific Party, 1994. Site 891. In Westbrook, G.K., Carson, B., Musgrave, R.J., et al., *Proc. ODP, Init. Repts.*, 146 (Pt. 1): College Station, TX (Ocean Drilling Program), 241–300.

Date of initial receipt: 1 September 1994

Date of acceptance: 24 March 1995

Ms 146SR-248

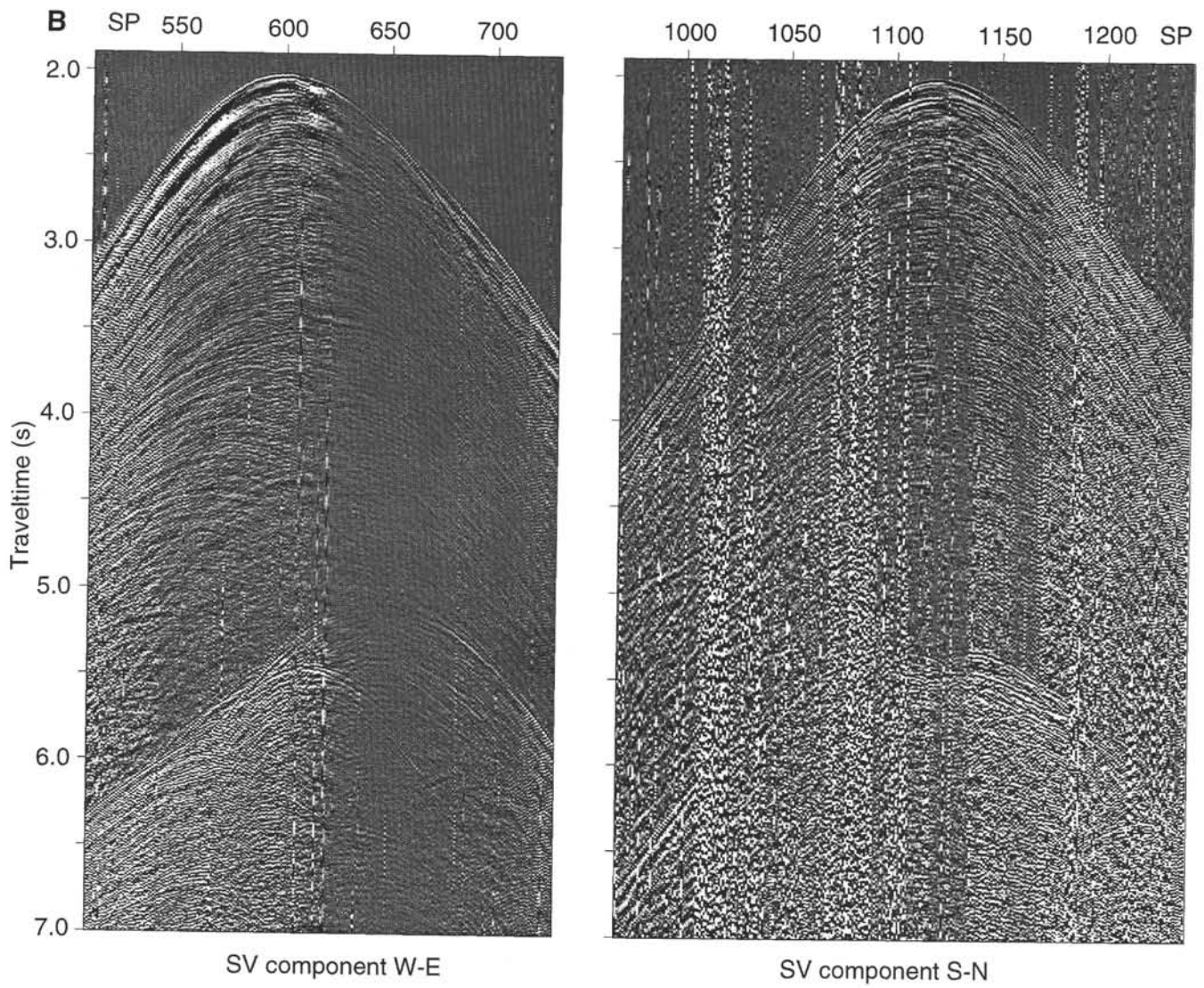


Figure 8 (continued).

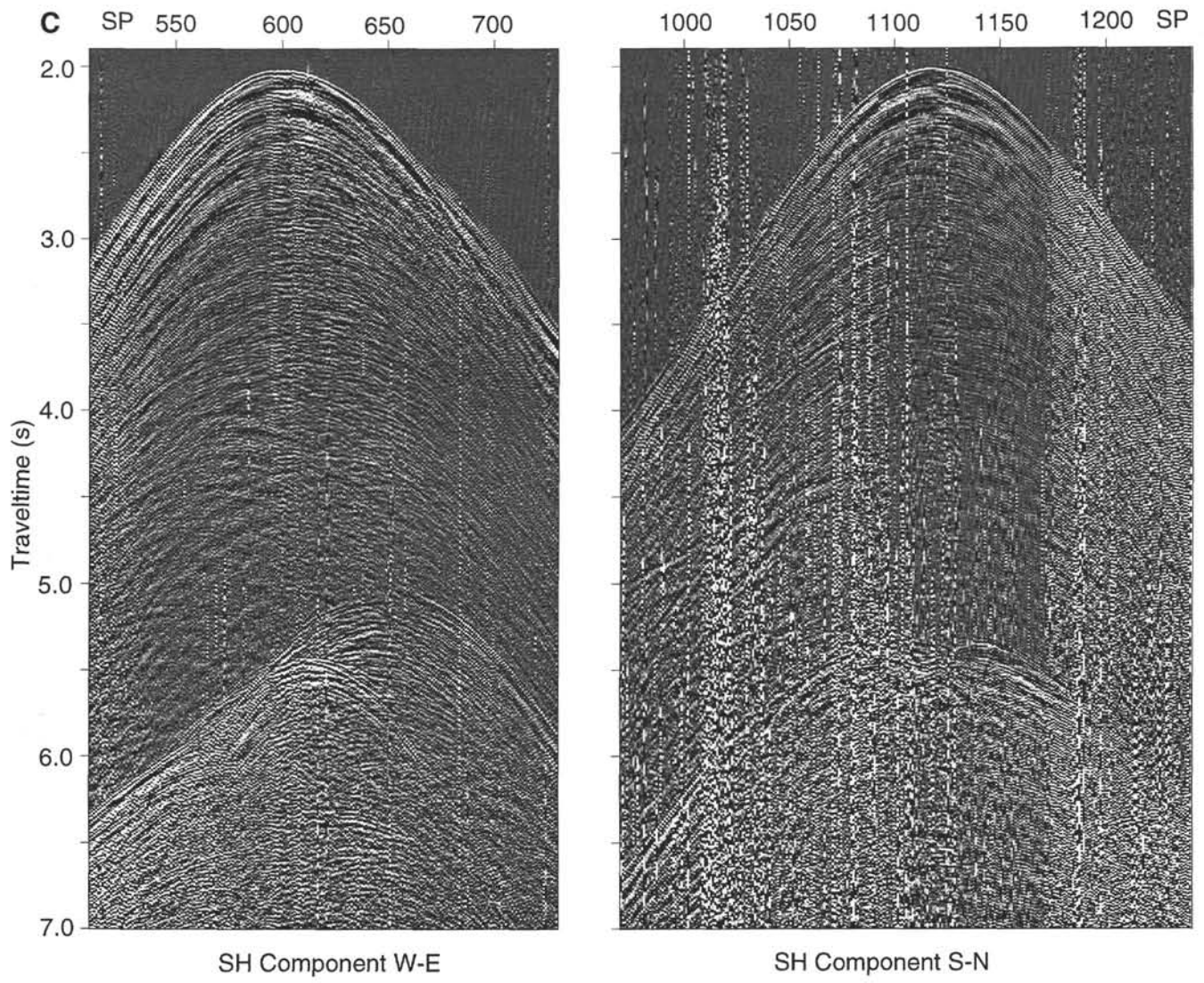


Figure 8 (continued).

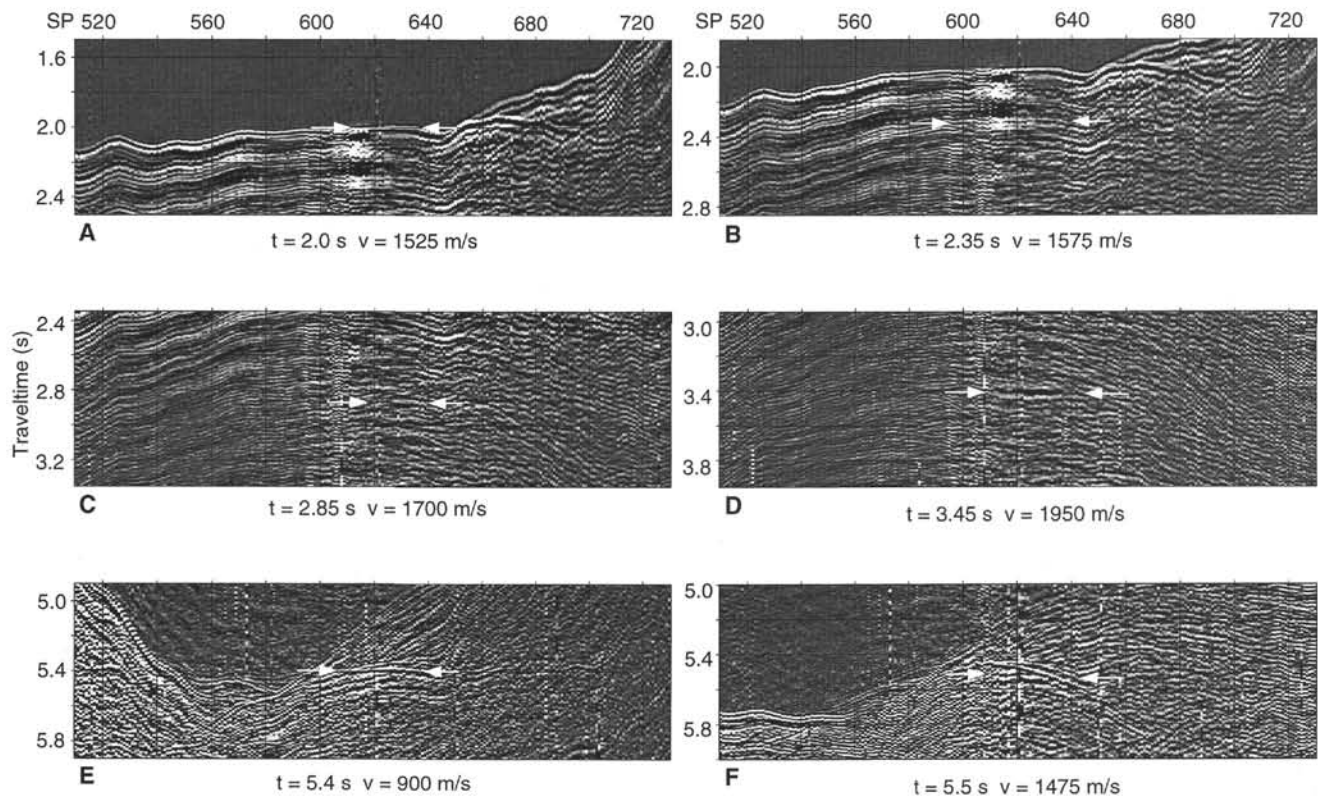


Figure 9. Walkaway VSP data along line 1 with RMS velocity applied. **A–D, F**, *P*-component. **E**, *SH* component. Flat events (shown between white arrows) are properly corrected with the indicated velocity. Deviations from the horizontal of indicated events are evidence of extreme lateral velocity heterogeneity.

Table 1. Walkaway VSP velocities.

Time (s)	Two-way traveltime (s)	Depth (mbsf)	RMS velocity (m/s)	Offset (m)	Interval velocity (m/s)	Interpretation
1.80	3.60	0	1480		1480	Seafloor
2.00	4.00	357	1525	0	1882	Earliest direct <i>P</i>
2.35	4.35	999	1575	0 E, -250 N	1835	
2.85	4.85	2096	1700	0 E, 250 N	2194	
3.45	5.45	3808	1950	250 E, 0 N	2853	
5.4			900	250 E, 250 N	340	Shear event

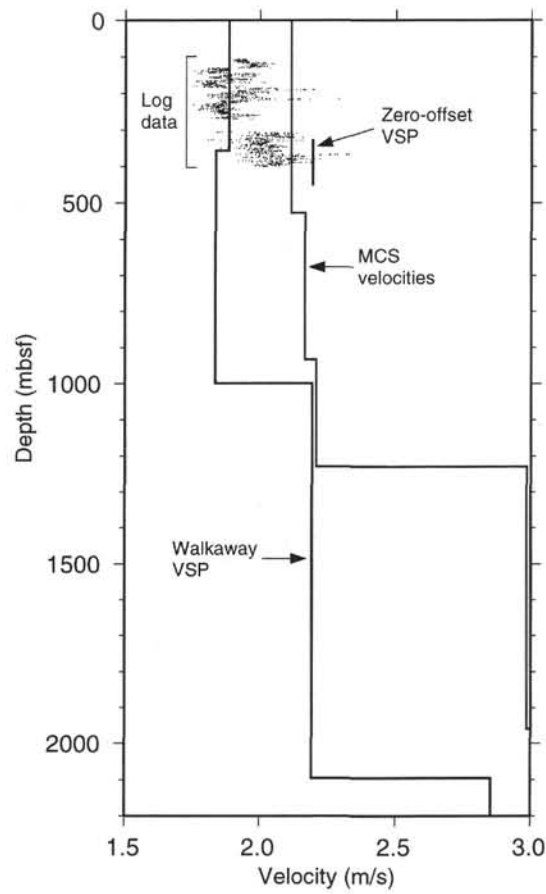


Figure 10. Comparison of velocity data from wire-line logging (all data points shown), MCS velocity analysis (Cochrane et al., 1994b), zero-offset VSP, and walkaway VSP.